

## Fréedericksz transition in an antclinic liquid crystal

Bing Wen,<sup>1</sup> Shiyong Zhang,<sup>1</sup> S. S. Keast,<sup>2</sup> M. E. Neubert,<sup>2</sup> P. L. Taylor,<sup>1</sup> and Charles Rosenblatt<sup>1</sup>

<sup>1</sup>Department of Physics, Case Western Reserve University, Cleveland, Ohio 44106

<sup>2</sup>Liquid Crystal Institute, Kent State University, Kent, Ohio 44242

(Received 6 June 2000)

The Fréedericksz geometry is used to show experimentally that a very-long-pitch, surface stabilized, antclinic liquid crystal undergoes a two-step electric-field-induced transition to the synclinic phase. The liquid crystal remains undistorted below the threshold field  $E_{th}$ . For  $E > E_{th}$ , a Fréedericksz transition occurs, wherein molecules in adjacent smectic layers undergo unequal azimuthal rotations about the layer normal, resulting in a nonzero polarization that couples to the applied field. Measurements of  $E_{th}$  as a function of temperature are reported. Related quasielastic light scattering measurements demonstrate that acoustic Goldstone mode fluctuations are quenched by a dc electric field  $E > E_{th}$ . At high fields a transition to the synclinic phase occurs *via* solitary waves.

PACS number(s): 61.30.Gd

Anticlinic liquid crystals are studied for their fundamental scientific interest as well as their potential for electrooptic devices [1,2]. In the anticlinic phase, also known as the smectic- $C_A^*$  phase, the director tilts by polar angle  $\theta$  with respect to the smectic layer normal (Fig. 1). Additionally, the azimuthal orientation of the director changes by  $\Delta\varphi \approx \pi$  from layer  $i$  to layer  $i+1$ . For a typical chiral anticlinic material,  $\Delta\varphi$  differs from  $\pi$  by typically 1% or 2%; on the other hand, for a pitch-compensated mixture where the helical pitch is infinite,  $\Delta\varphi$  is identically equal to  $\pi$ . Thus, for typical chiral anticlinic materials, the director is arranged in a double helix—one helix for the odd-numbered layers and another for the even-numbered layers—whose identical pitches are typically several hundreds of smectic layers. In each layer there is a polarization  $\vec{P}$  that lies perpendicular to the molecular tilt plane, where the azimuthal orientation of  $\vec{P}$  also rotates by  $\Delta\varphi$  from one layer to the next (Fig. 1). For a finite helical pitch the polarizations in adjacent layers are not quite antiparallel, and a local nonzero average polarization is obtained. Thus, when subjected to a weak electric field, the helices distort [3], giving rise to a small change in the transmitted light intensity when the cell is placed between a pair of crossed polarizers. Above some higher critical field  $E_{s.w.}$  there is a discontinuous transition from the distorted anticlinic phase to the synclinic phase (the smectic- $C^*$  phase, Fig. 1), such that the azimuthal orientation of the director is spatially uniform and all layer polarizations are parallel to the applied field. Associated with this field-induced transition, which occurs by fingerlike solitary waves [4], is a large change in the transmitted light intensity.

For very-long-pitch, surface-stabilized, anticlinic liquid crystals, the behavior at small electric fields is expected to be considerably different. For this situation it is possible to achieve an infinite-pitch helix, i.e., near-perfect bookshelf alignment (see Fig. 1), so that  $\Delta\varphi = \pi$  and the tilt plane of the molecules lies everywhere parallel to the plane of the cell; this was demonstrated using mixtures of MHPBC and TFMHPBC [5]. Qian and Taylor have predicted [6] that,

instead of a continuous variation of the director orientation with field beginning at  $E=0$ , a sharp Fréedericksz transition would occur in an infinite-helical-pitch anticlinic liquid crystal, where the electric field is oriented perpendicular to the molecular tilt plane. The Fréedericksz transition is a well-known phenomenon in nematic liquid crystals [7], where the elastic force favors a uniform structure and the electric field attempts to distort the structure. As both terms in the nematic free energy have the same quadratic dependence on the angle made by the molecular director with the surface-imposed “easy axis,” a sharp orientational transition occurs when the electric field is sufficiently large to overcome the elastic force. For the case of the anticlinic Fréedericksz transition, there are *three* dominant forces, viz., a linear coupling between  $\vec{P}$  and  $\vec{E}$ , a long-wavelength splay elastic force, and the anticlinic force that favors  $\Delta\varphi = \pi$ . For  $E < E_{th}$ , where  $E_{th}$  is the Fréedericksz threshold field, the splay elasticity and the anticlinic interactions dominate the free energy, and the rigid anchoring of the director at the two substrates precludes any elastic distortion. For  $E > E_{th}$ , the electric field overcomes both the elasticity and the anticlinic interactions: The polarizations in adjacent layers experience a torque from the electric field, causing molecules in adjacent layers to undergo unequal azimuthal rotations. The rotation in each

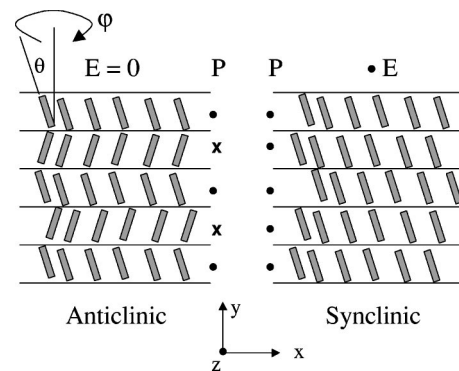


FIG. 1. Schematic representation of anticlinic (smectic  $C_A^*$ ) phase (left) for an infinitely long helical pitch at electric field  $E = 0$ . The angle  $\theta$  describes the polar tilt of the molecules and  $P$  the layer polarization. For sufficiently large electric field  $E$ , a transition to a synclinic (smectic  $C^*$ ) phase (right) occurs.

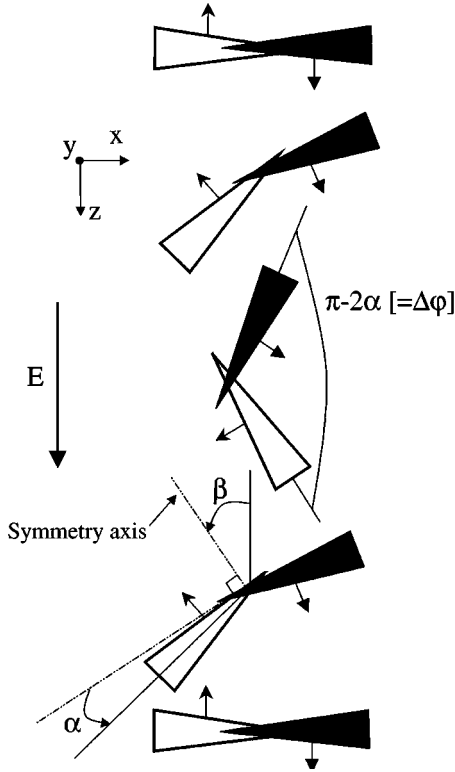


FIG. 2. Schematic representation of projection of molecular directors into the  $xz$  plane for two adjacent smectic layers when  $E > E_{th}$ . All black molecules lie in one smectic layer, and all white molecules lie in the smectic layer immediately below. Layer normal is along the  $y$  axis. Molecules are assumed to remain anchored at the walls. “Symmetry axis” corresponds to the symmetry axis of the director projections for a pair of molecules in two successive smectic layers. Angle  $\beta$  corresponds to the average azimuthal rotation of the symmetry axis from its undisturbed value at  $E=0$ ; angle  $\alpha$  corresponds to the deviation from perfect anticlinic order. Arrows correspond to the layer polarization, which is locally perpendicular to the molecular tilt plane.

layer, as well as the quantity  $|\Delta\varphi - \pi|$ , are maximum in the center of the cell, and go to zero at the two substrates if the anchoring is rigid. At a much higher field  $E_{s.w.}$ , the distorted anticlinic order switches discontinuously to synclinc order by means of solitary waves, analogous to the solitary-wave behavior observed in short-helical-pitch materials [4]. In this paper we demonstrate experimentally the low-field Fréedericksz switching mechanism in an anticlinic liquid crystal using an ac electric field, and measure its behavior with temperature. We find that the threshold field  $E_{th}$  is proportional to  $d^{-1}$ , where  $d$  is the cell thickness, and is of the same order as that predicted by theory. Additionally, we examine the fluctuations of the acousticlike Goldstone mode as a function of the applied dc field above the Fréedericksz threshold, finding an increase in the *inverse* relaxation time  $\tau_{\beta}^{-1}$  that is consistent with a quenching of fluctuations in  $\vec{P}$ . A preliminary account of part of this work has been presented in Ref. [8].

Let us first consider a simple model. For the geometry in Fig. 2, the bulk free energy  $F$  for a pair of adjacent layers may be written

$$F = WL \int_0^d dz \left\{ PE[\cos(\beta + \alpha) - \cos(\beta - \alpha)] + \frac{1}{2}B \left[ \left[ \frac{\partial(\beta - \alpha)}{\partial z} \right]^2 + \left[ \frac{\partial(\beta + \alpha)}{\partial z} \right]^2 \right] + 2U(1 - \cos 2\alpha) - \frac{\Delta\varepsilon \sin^2\theta}{8\pi} E^2 [\cos^2(\beta - \alpha) + \cos^2(\beta + \alpha)] \right\}, \quad (1)$$

where azimuthal rotation angles  $\alpha$  and  $\beta$  are functions of  $z$ , the axis perpendicular to the cell walls. Here  $L$  is the layer spacing,  $W$  is the width of the cell,  $\beta$  is the azimuthal rotation of the symmetry axis for a pair of molecules in adjacent layers, and  $\alpha$  is half the deviation from perfect anticlinic order, i.e.,  $\alpha = \frac{1}{2}(\pi - \Delta\varphi)$ . Additionally,  $U$  is the interaction coefficient associated with deviations from anticlinic order [9], i.e., deviations from  $\alpha=0$ ;  $B = K_{11} \sin^2\theta$ , where  $K_{11}$  is the splay elastic constant; and  $\Delta\varepsilon$  is the dielectric anisotropy. [Note that in Eq. (1) of Ref. [8] there was a pair of sign errors, which have been corrected above. Additionally, we have changed the notation for the elastic constant (scaled by  $\sin^2\theta$ ) from  $K$  in Ref. [8] to  $B$  in this paper.] The dielectric term is about two orders of magnitude smaller than the polarization term, and henceforth will be neglected. Minimization of this free energy results in a pair of coupled nonlinear Euler-Lagrange equations for which no analytic solution exists [6]. In the vicinity of the Fréedericksz transition, however, the values of  $\alpha(z)$  and  $\beta(z)$  will be small, and we can then expand  $F$  in powers of  $\beta$  and  $\alpha$  to quadratic order and obtain

$$F \approx WL \int_0^d dz \left\{ -2PE\alpha\beta + B \left( \left[ \frac{\partial\alpha}{\partial z} \right]^2 + \left[ \frac{\partial\beta}{\partial z} \right]^2 \right) + 4U\alpha^2 \right\}. \quad (2)$$

If we assume strong anchoring, which requires that  $\beta$  and  $\alpha$  vanish at the two surfaces, we may substitute the Fourier expansion  $\beta = \sum_q \beta_q \sin qz$  and  $\alpha = \sum_q \alpha_q \sin qz$  into  $F$ , where the wave vector  $q = q_z = \pi j/d$  and  $j$  is an integer. The free energy then becomes the sum of independent contributions from the separate Fourier components, each of which is a quadratic form in  $\alpha_q$  and  $\beta_q$ . Because the elastic energy increases quadratically with  $q$ , only the smallest value  $q = \pi/d$  need be retained. The threshold electric field  $E_{th}$  is the field at which the quadratic form first exhibits a negative eigenvalue, and is given by  $E_{th} = (\pi/Pd) \sqrt{B(4U + B\pi^2/d^2)}$ . As the term  $4U \gg B\pi^2/d^2$ , we may approximate  $E_{th}$  as

$$E_{th} \approx \frac{2\pi}{d} \sqrt{\frac{UB}{P^2}}. \quad (3)$$

Below this threshold the free energy is minimized only when  $\alpha_q = \beta_q = 0$ . For  $E > E_{th}$  the values of  $\alpha_q$  and  $\beta_q$  would grow without limit, and so we must restore the dominant fourth-order term in  $F$ . We then find that for  $E > E_{th}$  we have  $\beta_q \approx 2\sqrt{(E - E_{th})/E_{th}}$ . Moreover, above the threshold field  $\beta_q = PE\alpha_q/Bq^2$ , and therefore  $\beta_q \gg \alpha_q$ . These rotations give rise not only to a change in the optical retardation, but to a

tilt of the optic axis as well. From Eq. (3) we find that the threshold voltage is independent of  $d$  and is given by

$$V_{\text{th}} = 2\pi \sqrt{\frac{UB}{P^2}}. \quad (4)$$

Two cells were prepared by cleaning two pairs of indium-tin-oxide coated glass slides, spin-coating the slides with polyimide RN1266 (Nissan Chemicals), and baking. The coated slides were then rubbed with a cotton cloth using a dedicated rubbing machine and placed together with the rubbing directions parallel, separated by Mylar spacers. The cells were then cemented, and the measured thicknesses of the two cells were  $(7 \pm 1)$  and  $(11 \pm 1)$   $\mu\text{m}$ . Following the work of Ref. [5], in which it was found that the helical pitch unwinds at a certain concentration in a mixture of R-MHPBC and R-TFMHPBC, we filled the cells in the isotropic phase with a binary mixture of the related materials (R)-TFMHPOBC [4-(1-trifluoromethylhexyloxy-carbonyl)phenyl 4'-octyloxybiphenyl 4-carboxylate] (Ref. [10]) and (R)-MHPOBC [4-(1-methylheptyloxycarbonyl)phenyl 4'-octyloxybiphenyl-4-carboxylate] (Ref. [1]). As noted by Li *et al.* [5], the polarizations add constructively, but their helices wind in opposite directions. We found that a 70:30 wt. % mixture of (R)-TFMHPOBC and (R)-MHPOBC provides an extremely long pitch that could easily be surface stabilized in the bookshelf geometry. Each cell was then slowly cooled through the isotropic–smectic- $A$  phase transition at  $138^\circ\text{C}$ , through the smectic- $A$ –smectic- $C_A^*$  transition at  $120^\circ\text{C}$ , and stabilized at  $113^\circ\text{C}$  in the anticlinic smectic- $C_A^*$  phase. A focused beam from a 5 mW He-Ne laser passed consecutively through a light chopper, a polarizer, a Babinet-Soleil compensator, the cell, an analyzer, and into a detector. The detector output was fed into a lock-in amplifier, which was referenced to the chopping frequency of  $\omega = 2004 \text{ s}^{-1}$  ( $f = 319 \text{ Hz}$ ), allowing us to measure the dc intensity in an illuminated room. The polarizer and analyzer were oriented at  $45^\circ$  with respect to the liquid crystal's optic axis at  $E = 0$ , which is perpendicular to the smectic layers. The compensator was adjusted in the absence of an applied field so that the total optical phase retardation  $\delta$  of the compensator and liquid crystal was  $\delta = 0$ , corresponding to a near zero intensity at the detector.

A dc electric field may be used to induce a Fréedericksz transition. However, because the electrical resistance of the thin polyimide layers was at least an order of magnitude larger than that of the liquid crystal—and both were larger than  $1 \text{ M}\Omega$ —the voltage drop across the polyimide layer would have been much larger than that across the liquid crystal. This is an undesirable situation, as it is difficult to determine accurately the applied dc field across the liquid crystal. On the other hand, for a sufficiently high-frequency ac field, the free charges in the cell are unable to follow the field. In this case the electric fields across the thin polyimide layers and across the much thicker liquid crystal region would be determined not by charge transfer, but rather by the dielectric constants and thicknesses of the layers. As the dielectric constant of the polyimide is comparable to that of the liquid crystal, and the liquid crystal layer is much thicker than the two polyimide layers, the ac field across the liquid

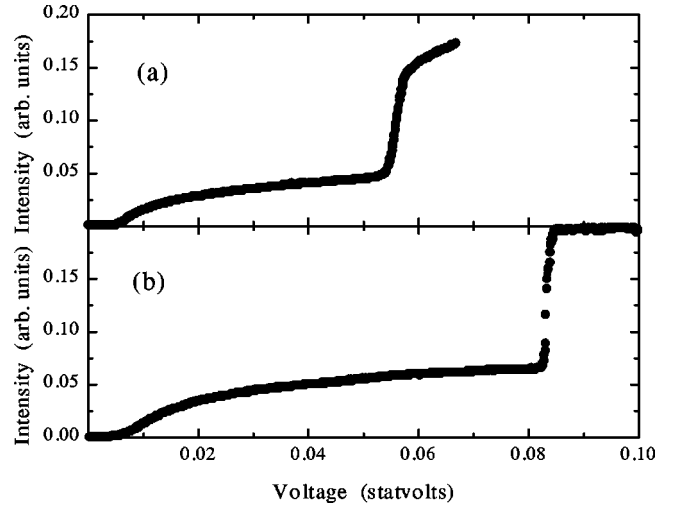


FIG. 3. Intensity vs voltage for (a) the  $d = 7 \mu\text{m}$  cell and (b) the  $d = 11 \mu\text{m}$  cell. Both Fréedericksz transitions occur at the same voltage, whereas solitary waves arise at the same field (and therefore at different voltages). Note that the intensity units are not the same in the two figures.

crystal could be taken as  $E \approx V/d$ . We thus chose to perform an ac experiment at frequency  $\omega$  larger than approximately  $30 \text{ s}^{-1}$  in order to avoid effects due to this motion of free charges. In order to simplify the interpretation of the results, the driving frequency must satisfy two further conditions. The rates of relaxation of the variables described by the angles  $\alpha$  and  $\beta$  are markedly different. The rate  $\Gamma_\alpha$  of decay of opticlike perturbations to  $\alpha$  is rather rapid, and is independent of  $q$  and represents short-range interactions between adjacent smectic layers. The relaxation rate  $\Gamma_\beta$  of acousticlike perturbations to  $\beta$ , on the other hand, is characteristic of the Fréedericksz transition: It is  $q_z$  dependent and is much slower. Using an in-plane field to drive the “optic mode” in which  $\alpha$  oscillates, we previously found [9] that  $\Gamma_\alpha$  is approximately  $5000 \text{ s}^{-1}$  for this mixture at  $T = 113^\circ\text{C}$ . The rate  $\Gamma_\beta$ , however, is only of the order of a few tenths  $\text{s}^{-1}$  near  $E_{\text{th}}$ , and vanishes at  $E_{\text{th}}$ . By choosing an angular frequency  $\omega$  for the applied field such that  $\Gamma_\alpha \gg \omega \gg \Gamma_\beta$ , it is possible to make an adiabatic approximation in which  $\alpha$  is assumed to follow instantaneously the time variation of  $E$ , but in which  $\beta$  is assumed to be constant. For an applied field of amplitude  $E_0$ , we have  $\alpha \propto E_0 \cos \omega t$  and  $\beta$  a constant determined by the time average of  $\alpha E$ . The expression for the threshold field  $E_{\text{th}} = (2\pi/d)\sqrt{UB/P^2}$  remains valid when  $E_{\text{th}}$  is interpreted as the root-mean-square field  $E_0/\sqrt{2}$ . In order to meet all three criteria, we have the condition that  $30 < \omega < 5000 \text{ s}^{-1}$ . We have therefore chosen  $\omega = 710 \text{ s}^{-1}$  (corresponding to  $f = 113 \text{ Hz}$ ) at which to perform the experiment.

Fréedericksz measurements were performed as a function of temperature in the anticlinic phase. The rms amplitude of the ac voltage was ramped from 0 to 0.08 statvolts at a rate of  $2.7 \times 10^{-5} \text{ statvolts s}^{-1}$ , and the detector intensity was computer recorded. Figure 3(a) shows a trace of the intensity  $I$  vs voltage for the  $d = 7 \text{ mm}$  cell at  $T = 113^\circ\text{C}$ , and Fig. 3(b) shows  $I$  for the  $d = 11 \text{ mm}$  cell. We note that, for our optical geometry, just above the Fréedericksz transition the intensity  $I$  is proportional to the square of the optical retar-

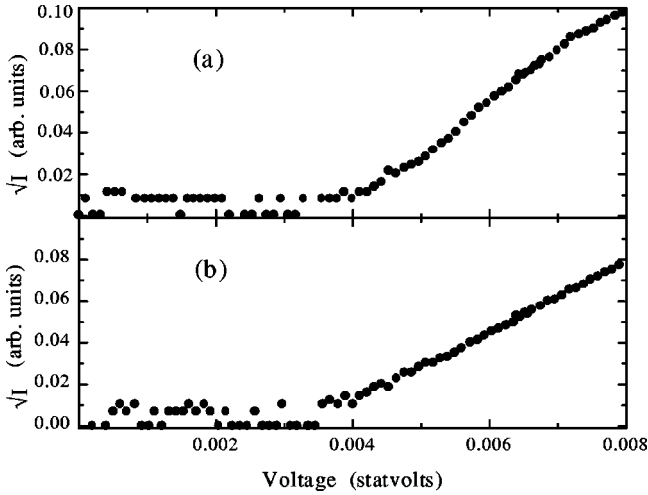


FIG. 4. The square root of the light intensity is shown as a function of voltage in the vicinity of the Fréedericksz transition for (a) the  $d=7 \mu\text{m}$  cell and (b) the  $d=11 \mu\text{m}$  cell. Note that for  $V < V_{\text{th}}$ , fluctuations in  $I^{1/2}$  are artificially accentuated because of the digital signal.

dation  $\delta^2$ , which in turn is proportional to  $\beta_q^4$ . Since according to Ref. [6],  $\beta_q \propto (V - V_{\text{th}})^{1/2}$ , we show in Fig. 4(a) the quantity  $I^{1/2}$  versus  $V$  in the vicinity of the threshold voltage  $V_{\text{th}}$  for the  $d=7 \text{ mm}$  cell, and in Fig. 4(b) we show  $I^{1/2}$  versus  $V$  for the  $d=11 \text{ mm}$  cell. The linear behavior for  $V > V_{\text{th}}$  allows us to extract the threshold voltage  $V_{\text{th}} = (0.0038 \pm 0.0004)$  statvolts for the  $d=7 \text{ mm}$  cell, and  $V_{\text{th}} = (0.0036 \pm 0.0004)$  statvolts for the  $d=11 \text{ mm}$  cell. The fact that the threshold voltages are the same is a clear indication of Fréedericksz behavior which, for moderately strong anchoring, predicts a thickness-independent threshold voltage. As an aside, we note that the experiment was also conducted at a higher frequency of  $\omega = 2000 \text{ s}^{-1}$ , with virtually identical results. Additionally, when the voltage was slowly swept downward, hysteresis was minimal.

Above the threshold voltage the intensity continues to increase, but at a slower rate, as both  $\beta_q$  and  $\alpha_q$  increase with field. Qian and Taylor predicted [6] that at a sufficiently large field a sharp transition to synclinc order would occur, where  $\beta_q = \alpha_q = \pi/2$ , but they did not theoretically examine the dynamics of this transition. Our observations using a polarizing microscope at a visually accessible driving frequency of  $\omega \approx 70 \text{ s}^{-1}$  reveal synclinc fingers, approximately  $10 \mu\text{m}$  in width, propagating along the smectic layers into the anticlinic region, and thus support this prediction. These fingers advance and retreat at frequency  $\omega$ , with  $\beta_q$  remaining fixed and  $\alpha_q$  changing sign at each field reversal. At our experimental frequency  $\omega = 710 \text{ s}^{-1}$  the finger reversal could not be detected by eye, although the intensity at the detector exhibited a sharp increase with voltage (Fig. 3). We found, for the  $d=7 \text{ mm}$  cell, a critical field  $E_{\text{s.w.}} = (77 \pm 7)$  statvolt  $\text{cm}^{-1}$  for the onset of solitary waves, which was similar to the value  $E_{\text{s.w.}} = (75 \pm 10)$  statvolts  $\text{cm}^{-1}$  found for the  $d=11 \text{ mm}$  cell. This behavior is consistent with a *field-dependent*, rather than voltage-dependent, solitary wave threshold [4]. The uncertainty in  $E_{\text{s.w.}}$  is due primarily to the uncertainty in cell thickness  $d$  rather than to an uncertainty in determining the voltage.

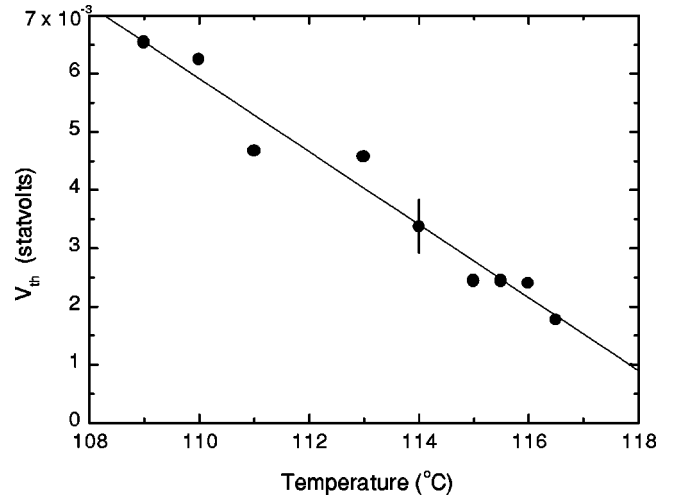


FIG. 5. Threshold voltage  $V_{\text{th}}$  vs temperature for a cell of thickness  $d = (12 \pm 1) \mu\text{m}$ .

In Fig. 5 we show the Fréedericksz threshold voltage  $V_{\text{th}}$  versus temperature  $T$  for a cell of thickness  $d = (12 \pm 1) \mu\text{m}$ . If we assume that the polarization  $P$  scales as  $\sin \theta$  and  $B$  scales as  $\sin^2 \theta$  [7], we would expect that  $V_{\text{th}} \propto U^{1/2}$  [Eq. (4)]. Data for  $U$  have been reported by Kimura *et al.* [9], who found that  $U$  exhibits a monotonic decrease with increasing temperature below the smectic-A–smectic- $C_A^*$  phase transition temperature  $T_{A-C_A^*}$ . Their experimental curve for  $U$  versus  $T - T_{A-C_A^*}$  appears to be somewhat ‘‘S’’-shaped [9], although the error bars are sufficiently large that a linear—or slower than linear—increase of  $U$  with  $T$  cannot be ruled out. In Fig. 6 we show the ratio  $V_{\text{th}}/U^{1/2}$ , which should be constant if our prediction is correct, as a function of  $T - T_{A-C_A^*}$ . Note that we have used linearly fitted values of  $V_{\text{th}}$ , rather than the actual data points shown in Fig. 5. Over most of the temperature range, values of this ratio lie between  $3$  and  $4 \times 10^{-5}$  statvolt  $\text{cm}^{3/2} \text{erg}^{-1/2}$ , falling within experimental error. Near the transition temperature, where  $V_{\text{th}}$  is difficult to determine, and for  $T - T_{A-C_A^*} > 10^\circ\text{C}$ , val-

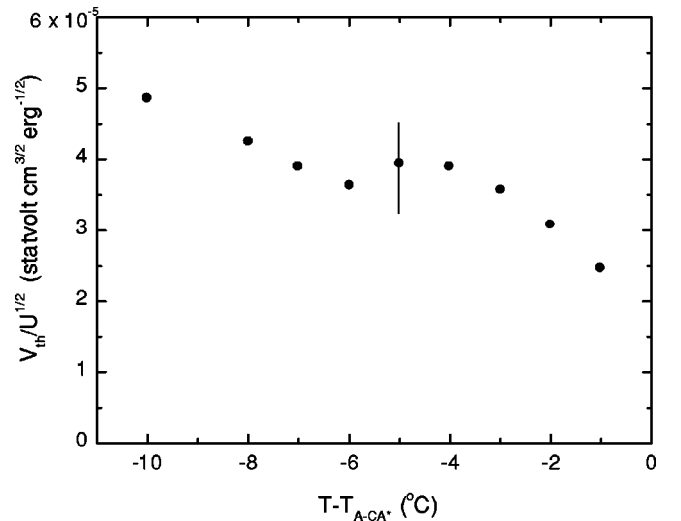


FIG. 6. Threshold voltage  $V_{\text{th}}$  divided by the square root of the anticlinic interaction parameter  $U$  as a function of temperature.



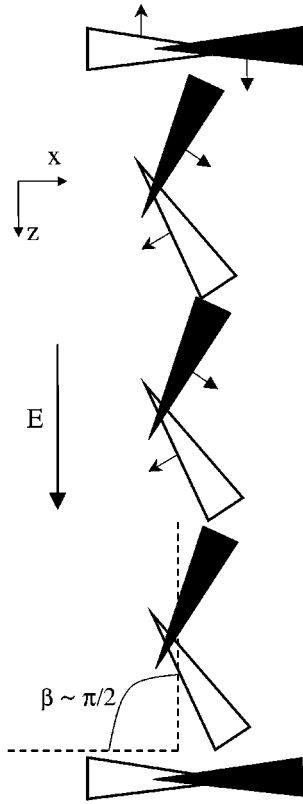


FIG. 7. Schematic view of molecules in adjacent layers (see caption in Fig. 1) for  $E \gg E_{th}$ .

ues for  $V_{th}/U^{1/2}$  differ a bit from those in the midtemperature region. However, all of these variations are smaller than the much larger variation of  $V_{th}$  with temperature (cf. Fig. 5). Thus, although not completely flat with temperature, the general behavior of  $V_{th}/U^{1/2}$  is moderately consistent with that expected.

Although the experimental results confirm the existence of a Fréedericksz transition, discrepancies exist between our results and the model. First, the model predicts that  $V_{th} = 2\pi\sqrt{UB/P^2}$ . For our material at  $T=113^\circ\text{C}$ , we previously measured [9]  $P=300\text{ esu cm}^{-2}$ ,  $U=2 \times 10^4\text{ erg cm}^{-3}$ , and  $\theta=22.5^\circ$ . If we assume that  $K_{11} = 1.5 \times 10^{-6}\text{ dyn}$ , corresponding to  $B=2.2 \times 10^{-7}\text{ dyn}$ , we would expect  $V_{th} \approx 0.0015\text{ statvolts}$ . However, the experimental values of  $V_{th}$  are approximately twice as large as those predicted by the simple theory. One possible explanation could be that our assumed value for  $K_{11}$  is too small, and that, due to interlayer correlations in the anticlinic phase,  $K_{11}$  is somewhat larger than our estimate. Some evidence for this conjecture was found in recent quasielastic light scattering experiments on this mixture [11], which examine the coupling between the acoustic and optic Goldstone modes as a function of applied dc electric field  $E^{dc}$ . In that experiment the actual value of  $E^{dc}$  was determined by comparing the ac Fréedericksz threshold voltage  $V_{th}^{ac}$  with its dc counterpart  $V_{th}^{dc}$ , viz.,  $E^{dc} = (V_{th}^{ac}/V_{th}^{dc})(V^{dc}/d)$ . From the data an elastic constant  $K_{11} \sim 2 \times 10^{-6}\text{ dyn}$  was deduced [11]. This figure is slightly larger than our estimate for  $K_{11}$ , although not enough to improve significantly the agreement of our Fréedericksz results with Eq. (4). An alternative reason for the larger-than-expected measured value of  $V_{th}$  may lie with the

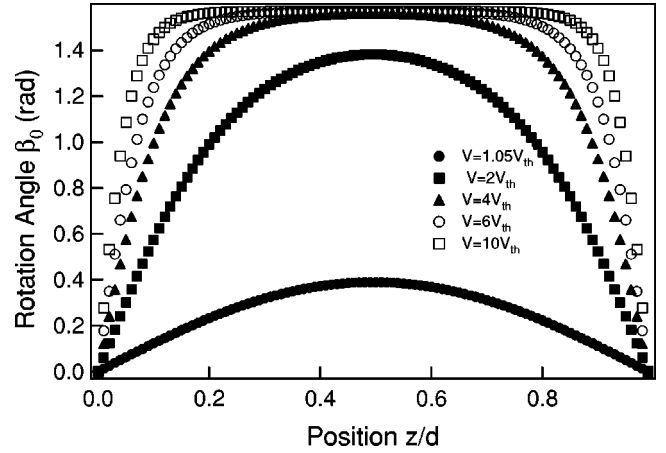


FIG. 8. Numerical computation of equilibrium angle  $\beta$  vs relative position in the cell of thickness  $d=12\ \mu\text{m}$  for various applied voltages.

simplicity of our model, which assumes two-layer periodicity and does not allow for next-nearest-neighbor interactions [12].

Another tool with which to explore the behavior of this material is dynamic light scattering in the presence of strong electric fields, for which  $E_{s.w.} > E \gg E_{th}$ . In this region of field  $\beta$  is nearly equal to  $\pi/2$  over most of the cell, except for a small coherence length near each of the two surfaces (see Fig. 7), and a strong electric field has the effect of quenching thermal fluctuations of the azimuthal orientation. We first calculated the profiles of  $\alpha$  and  $\beta$  across the cell as functions of voltage using Eq. (1) for a cell of thickness  $d=(12 \pm 1)\ \mu\text{m}$ . The required parameters for the calculation were taken to be  $P=300\text{ esu cm}^{-2}$ ,  $U=2 \times 10^4\text{ erg cm}^{-3}$ , and the one-elastic constant approximation  $B=2.2 \times 10^{-7}\text{ dyn}$ ; rigid anchoring conditions were assumed. In Fig. 8 we show the calculated equilibrium angle  $\beta$  along the  $z$  axis, perpendicular to the substrates, for several values of applied dc voltage  $V^{dc}$  relative to the dc threshold voltage  $V_{th}^{dc}$ . Note that  $V^{dc} = E^{dc}d$ , where  $E^{dc}$  has been defined above. For  $V^{dc} = 4V_{th}^{dc}$  we find that the coherence length (at the substrates) is approximately  $0.2d$ , or  $\sim 2\ \mu\text{m}$ , and that for  $V^{dc} = 10V_{th}^{dc}$  the length is  $\sim 1\ \mu\text{m}$ . Thus,  $\sim 65\%$  of the cell is reasonably well oriented with  $\beta \approx \pi/2$  for the first case, and  $\sim 85\%$  of the cell is well oriented for the second case. We have also theoretically examined the profile of  $\beta$  vs  $z/d$  for other values of  $P$ ,  $U$ , and  $B$ , finding that the results are very insensitive to these parameters for a given  $V/V_{th}$ .

For sufficiently large electric field, therefore, we may safely assume that  $\beta \approx \pi/2$  over most of the cell, and measure fluctuations in the refractive index that give rise to scattered light. These fluctuations are indicative of the deviations of  $\alpha$  and  $\beta$  from their equilibrium values, and the rate of decay of the time autocorrelation function of the scattered intensity corresponds to the relaxation time of these orientational fluctuations. Thus, by judicious choice of experimental geometry we may determine the relaxation time that is characteristic of each of the two modes. In particular, we have chosen to examine the relaxation time  $\tau_\beta$ , which is characteristic of acousticlike fluctuations in  $\beta$ , because of its experimental accessibility compared to fluctuations in  $\alpha$ .

Light from an argon-ion laser at wavelength  $\lambda=488\text{ nm}$

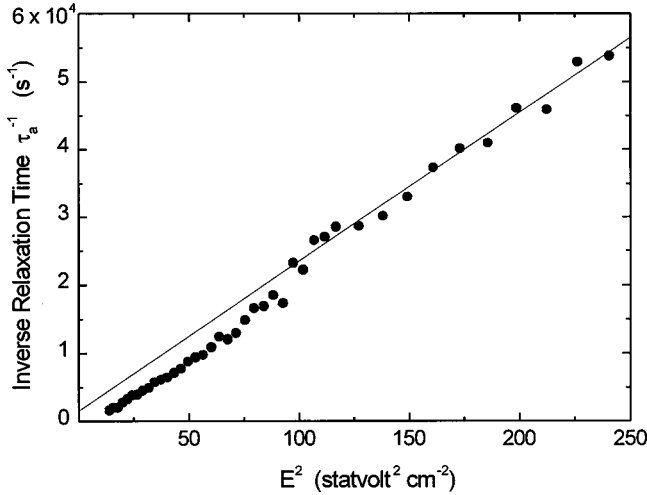


FIG. 9. Inverse relaxation time  $\tau_{\beta}^{-1}$  vs  $(E^{dc})^2$ .

was incident at an angle of  $33^\circ$  to the cell normal in the  $y$ - $z$  plane, where the incident optical polarization was along the  $x$  axis and the smectic layers lie in the  $x$ - $z$  plane. Depolarized scattered light (with the optical polarization in the  $y$ - $z$  plane) was detected by a photomultiplier tube at angle  $41^\circ$  to the cell normal, corresponding approximately to changes in wave number  $q_y = 1.4 \times 10^4 \text{ cm}^{-1}$  and  $q_z = 7.2 \times 10^3 \text{ cm}^{-1}$  [13]. The photocurrent passed into a pulse-amplifier-discriminator and into a Brookhaven Instruments model BI-9000 digital autocorrelator. Details of the experimental apparatus are given elsewhere [14]. Because the optic mode does not couple to the incident  $x$  polarization, we experimentally exclude optic mode ( $\alpha$ ) fluctuations from the signal. On the other hand, the acoustic mode couples the  $x$  and  $z$  optical polarizations. Thus, only the acoustic mode ( $\beta$ ) fluctuations and its attendant relaxation time  $\tau_{\beta}$  are probed in our geometry, where  $\tau_{\beta}$  is measured in the heterodyne mode because of the presence of static defects in the liquid crystal. The inverse relaxation times  $\tau_{\beta}^{-1}$  at  $T = 111^\circ \text{C}$  are plotted in Fig. 9, where it is seen that  $\tau_{\beta}^{-1}$  is approximately linear in  $(E^{dc})^2$ , especially for larger  $E^{dc}$ .

We can understand this result in the following way. We introduce the notation  $\alpha_o$  and  $\beta_o$  for the dc electric-field-dependent equilibrium angles  $\alpha$  and  $\beta$  in the interior of the cell, i.e., at  $z = d/2$ . Additionally, we introduce  $\Delta\alpha_{\vec{q}}$  and  $\Delta\beta_{\vec{q}}$  as the Fourier components of thermal fluctuations about these equilibrium angles. (Note that the momentum change, i.e., wave vector  $\vec{q}$ , need not be along the  $z$  axis for this experiment, although we confine  $\vec{q}$  experimentally to the  $y$ - $z$  plane.) Additionally, when  $\beta_o \approx \pi/2$ , we find to lowest order in  $\Delta\alpha_{\vec{q}}$  and  $\Delta\beta_{\vec{q}}$  that the  $\vec{q}$ -dependent free energy density for a pair of layers is

$$F_q^- = -2PE^{dc} \sin \alpha_o + \frac{1}{2}PE^{dc} \sin \alpha_o (\Delta\alpha_{\vec{q}}^2 + \Delta\beta_{\vec{q}}^2) + 2U(1 - \cos 2\alpha_o) + 8U \cos 2\alpha_o (\Delta\alpha_{\vec{q}}^2) + \frac{1}{2}B_y q_y^2 (\Delta\alpha_{\vec{q}}^2 + \Delta\beta_{\vec{q}}^2) + \frac{1}{2}B_z q_z^2 (\Delta\alpha_{\vec{q}}^2 + \Delta\beta_{\vec{q}}^2), \quad (5)$$

where  $B_y$  and  $B_z$ , which both scale as  $\sin^2 \theta$ , are elastic constants for distortions along the  $y$  and  $z$  axes, respectively. The equilibrium value  $\alpha_o$  may be obtained by neglecting the fluctuation terms and setting  $\partial F_q^- / \partial \alpha_o = 0$ , whence  $\alpha_o = \arcsin(PE^{dc}/4U)$ . Because only the acoustic-mode fluctuations  $\Delta\beta_{\vec{q}}$  are measured in this experiment, we drop the terms in  $\Delta\alpha_{\vec{q}}$  and find the contribution of fluctuations in  $\beta$  to the free energy to be

$$\Delta F_q^- = \frac{P^2 (E^{dc})^2}{8U} \Delta\beta_{\vec{q}}^2 + \frac{1}{2}B_y q_y^2 \Delta\beta_{\vec{q}}^2 + \frac{1}{2}B_z q_z^2 \Delta\beta_{\vec{q}}^2. \quad (6)$$

The relaxation time  $\tau_{\beta}$  of the acoustic eigenmode is thus given by

$$\tau_{\beta} = \frac{2\eta}{\{P^2 (E^{dc})^2 / 4U\} + B_y q_y^2 + B_z q_z^2}, \quad (7)$$

where  $\eta$  is a viscosity. Thus, for sufficiently large electric fields such that  $\beta_o$  is approximately  $\pi/2$ , the relaxation rate  $\tau_{\beta}^{-1}$  is predicted to be quadratic in the electric field. As seen in Fig. 9, this dependence is in agreement with our observations. In particular, extrapolation of the data at large  $(E^{dc})^2$  in Fig. 9 results in a small but positive value of  $\tau_{\beta}^{-1}$  at zero field, as expected. [Note that the data at small fields are not consistent with Eq. (7) because  $\beta$  cannot be approximated as  $\pi/2$  throughout the cell (cf. Fig. 8)]. Thus, in the limit of  $E \gg E_{th}$ , the same model that predicts a Fréedericksz transition may be used self-consistently to predict the electric field dependence of the light scattering.

To summarize, we have demonstrated that a Fréedericksz transition occurs at low voltages in a very-long-pitch, surface-stabilized anticlinic liquid crystal if the voltage is increased sufficiently slowly with time. Following this, a first-order transition occurs at higher fields to the synclinc state. We have thus confirmed that the switching mechanism from the anticlinic to synclinc orientation is actually a two-step process involving a Fréedericksz transition followed by solitary waves.

The authors are indebted to T. Qian, X.-Y. Wang, and R. G. Petschek for useful conversations. This work was supported by the National Science Foundation under Grant Nos. DMR-9982020 and DMR-0072935, and by the National Science Foundation's Advanced Liquid Crystalline Optical Materials Science and Technology Center (Grant No. DMR-8920147).

- [1] A.D.L. Chandani, T. Hagiwara, Y. Suzuki, Y. Ouchi, H. Takezoe, and A. Fukuda, *Jpn. J. Appl. Phys., Part 2* **27**, L729 (1988).  
 [2] A. Fukuda, Y. Takanishi, T. Isozaki, K. Ishikawa, and H. Takezoe, *J. Mater. Chem.* **4**, 997 (1994).

- [3] Y.P. Panarin, O. Kalinovskaya, and J.K. Vij, *Liq. Cryst.* **25**, 241 (1998).  
 [4] J.F. Li, X.Y. Wang, E. Kangas, P.L. Taylor, C. Rosenblatt, Y. Suzuki, and P.E. Cladis, *Phys. Rev. B* **52**, 13 075 (1995).  
 [5] J. Li, H. Takezoe, A. Fukuda, and J. Watanabe, *Liq. Cryst.* **18**,

- 239 (1995).
- [6] T.Z. Qian and P.L. Taylor, *Phys. Rev. E* **60**, 2978 (1999).
- [7] P.G. DeGennes and J. Prost, *The Physics of Liquid Crystals* (Clarendon, Oxford, 1994).
- [8] S. Zhang, B. Wen, S.S. Keast, M.E. Neubert, P.L. Taylor, and C. Rosenblatt, *Phys. Rev. Lett.* **84**, 4140 (2000).
- [9] M. Kimura, D.S. Kang, and C. Rosenblatt, *Phys. Rev. E* **60**, 1867 (1999).
- [10] Y. Suzuki, T. Hagiwara, I. Kawamura, N. Okamura, T. Kitazume, M. Kakimoto, Y. Imai, Y. Ouchi, H. Takezoe, and A. Fukuda, *Liq. Cryst.* **6**, 167 (1989).
- [11] S. Zhang, S.S. Keast, M.E. Neubert, R. G. Petschek, and C. Rosenblatt, *Phys. Rev. E* **62**, 5911 (2000).
- [12] M. Yamashita, *J. Phys. Soc. Jpn.* **65**, 2122 (1996).
- [13] Because the cell is thin,  $q_z$  actually depends on cell thickness.
- [14] G.A. DiLisi, C. Rosenblatt, A.C. Griffin, and U. Hari, *Phys. Rev. A* **45**, 1065 (1992).